Anomalous patterned scattering spectra of one-dimensional porous silicon photonic crystals

M. B. de la Mora,[1,*] J. A. del Río,[1,5] R. Nava,[1] J. Tagüeña-Martínez,[1] J. A. Reyes-Esqueda,[2] A. Kavokin,[3] J. Faubert,[4] and J. E. Lugo[4]

[1]*Centro de Investigación en Energía, Universidad Nacional Autónoma de México Privada Xochicalco S/N, Temixco, 62580 Morelos, México*
[2]*Instituto de Física, Universidad Nacional Autónoma de México. Circuito de la Investigación Científica Ciudad Universitaria, 04510 México, D. F. México*
[3]*School of Physics and Astronomy, University of Southampton Highfield, Southampton SO17 1BJ, UK*
[4]*Visual Psychophysics and Perception Laboratory, School of Optometry, University of Montreal, Montreal, H3C3J7 Canada*
[5]*Also in Centro de Ciencias de la Complejidad, Universidad Nacional Autónoma de México*

*mbmom@cie.unam.mx

Abstract: Far-field secondary emission spectra of free standing samples of one-dimensional porous silicon photonic crystals show characteristic co-focal rings centered close to the structure normal plane. The rings appear when the frequency of picoseconds excitation laser pulses is tuned into the edges of the fourth photonic band gap. They can be clearly distinguished from the typical reflected and transmitted light for an oblique incidence geometry. The rings number depends on the excitation frequency and the incidence angle. We explain these anomalous spectral features of porous silicon structures by the spectral filtering of light elastically scattered inside the photonic structure by the narrow photonic bands. The elastic scattering of light due to the photonic disorder in the structure causes the appearance of secondary waves propagating in any direction. But only those waves which fall into the allowed photonic bands may penetrate through the whole structure and move through its front or back surfaces. The observed patterned secondary emission is an example of efficient photonic engineering by simple means of multilayer porous silicon structures.

OCIS codes: (160.2710) Materials; (260.2030) Physical optics.

References and links

1. E. Yablonovitch, "Photonic band-gap structures," J. Opt. Soc. Am. B **2**, 283–295 (1993).
2. H. Kosaka, T. Kawashima, A. Tomita, M. Notomi, T. Tamamura, T. Sato, and S. Kawakami, "Superprism phenomena in photonic crystals," Phys. Rev. B **58**, 10096–10099 (1998).
3. E. Cubukcu, K. Aydin, E. Ozbay, S. Foteinopoulou, and C. M. Soukoulis, "Negative refraction by photonic crystals," Nature **423**, 604–605 (2003).
4. M. Notomi, "Theory of light propagation in strongly modulated photonic crystals: Refractionlike behavior in the vicinity of the photonic band gap," Phys. Rev. B **62**, 10696–10705 (2000).
5. B. Gralak, S. Enoch, and G. Tayeb, "Anomalous refractive properties of photonic crystals," J. Opt. Soc. Am. A **17**, 1012–1020 (2000).
6. W. Bogaerts, P. Bienstman, D. Taillaert, R. Baets, and D. De Zutter, "Out-of-plane scattering in photonic crystals," IEEE Photon. Technol. Lett. **13**, 565–567 (2001).

#133401 - $15.00 USD Received 16 Aug 2010; revised 22 Sep 2010; accepted 28 Sep 2010; published 13 Oct 2010

7. P. C. Ingrey, K. I. Hopcrafta, and E. Jakemana, "Negative refraction and rough surfaces: A new regime for lensing," Opt. Commun. **283**, 1188–1191 (2010).
8. V. Agarwal, J. A. del Río, G. Malpuech, M. Zamfirescu, A. Kavokin, D. Coquillat, D. Scalbert, M. Vladimirova, and B. Gil, "Photonic Bloch Oscillations in porous silicon optical superlattices," Phys Rev. Lett. **92**, 097401 (2004).
9. R. Nava, J. Tagüeña-Martínez, J. A. del Río, and G. G. Naumis, "Perfect light transmission in Fibonacci arrays of dielectric multilayers," J. Phys. Condens. Matter **21**, 155901–155906 (2009).
10. J. E. Lugo, B. de la Mora, R. Doti, R. Nava, J. Tagüeña, A. del Río, and J. Faubert, "Multiband negative refraction in one-dimensional photonic crystals," Opt. Express **17**, 3042–3051 (2009).
11. Z. Wei, H. Li, C. Wu, Y. Cao, J. Ren, Z. Hang, H. Chen, D. Zhang, and C. T. Chan, "Anomalous reflection from hybrid metamaterial slab," Opt. Express **18**, 12119–12126 (2010).
12. M. Gerken and D. A. B. Miller, " Wavelength demultiplexer using the spatial dispersion of multilayer thin-film structures," IEEE Photon. Technol. Lett. **15**, 1097–1099 (2003).
13. V. Agarwal and J. A. del Río, "Filters, mirrors and microcavities from porous silicon," Int. J. Mod. Phys. B **20**, 99–110 (2006).
14. A. G. Cullis, L. T. Canham, and P. D. J. Calcott, "The structural and luminescence properties of porous silicon," J. Appl. Phys. **82**, 909–965 (1997).
15. O. Bisi, S. Ossicini, and L. Pavesi, "Porous silicon: a quantum sponge structure porous silicon based optoelectronics," Surf. Sci. Rep. **38**, 1–126 (2000).
16. P. M. Fauchet, L. Tsybeskov, C. Peng, S. P. Duttagupta, J. von Behren, Y. Kostoulas, J. M. V. Vandyshev, and K. D. Hirschman, "Light-emitting porous silicon: materials science, properties, and device applications," IEEE J. Sel. Top. Quantum Electron. **1**, 1126–1139 (1995).
17. A. Kavokin, G. Malpuech, and I. Shelykh, "Negative refraction of light in Bragg mirrors made of porous silicon," Phys. Lett. A **339**, 387–392 (2005).
18. Y. Kanemitsu, H. Uto, and Y. Masumoto, "Microestructure and optical properties of free-standing porous silicon films: size dependence of absortion spectra in Si nanometer-sized crystallites," Phys. Rev. B **4**, 2827–2830 (1993).
19. M. B. de la Mora, O. A. Jaramillo, R. Nava, J. Tagüeña-Martínez, and J. A. del Río, "Viability study of porous silicon photonic mirrors as secondary reflectors for solar concentration systems," Sol. Energy Mater. Sol. Cells **93**, 1218–1224 (2009).
20. P. Yeh, "Bloch waves and band structures," in *Optical Waves in Layered Media*, (Whiley-Interscience Publication, 1988), pp. 119-134.
21. F. García-Santamaría, J. F. Galisteo-López, P. V. Braun, and C. López, "Optical diffraction and high-energy features in three-dimensional photonic crystals," Phys. Rev. B. **71**, 95112–95117 (2005).

1. Introduction

Photonic crystals (PC) are periodic structures which enable controlling the propagation of light [1]. In a PC light travels as Bloch waves and its propagation is mainly influenced by the PC's photonic band structure. Atypical light propagation in PC, close to the band gaps, including the superprism effect [2] and negative refraction behavior [3, 4, 5], has been reported by several authors. For a better understanding of this kind of anomalous behaviors, it is important to consider the effect of the imperfections in the PC periodic structure, which produce light scattering. Even perfect photonic slabs can show intrinsic scattering losses when the Bloch modes are not fully confined [6]. In spite of the scattering losses, sometimes it is possible to take advantage of the imperfections in PC for engineering optical applications as lenses [7]. In this work, we analyze the transmission behavior of light at the edges of the fourth photonic band gap in a Bragg mirror, which is the simplest one-dimensional photonic crystal (1D PC) made of porous silicon (p-Si) [8, 9]. Recently, we performed an experiment in one of these structures which gave some hints of an anomalous transmission [10]. In such experiments, the 1D PC of p-Si was on a crystalline silicon base. We decided to improve those results by using this time free standing samples. Here, we consider not just the peculiarities of the behavior of light close to the edge of photonic band gaps, but also the influence of the inhomogeneities in our 1D PC. Even if we have a 1D PC with high optical quality, some inhomogeneities due to the roughness are present, modifying the transmission of light by elastic scattering. This produces secondary waves propagating isotropically. Only those ones which belong to the allowed photonic bands would penetrate through the whole structure and move to its front or back surfaces.

#133401 - $15.00 USD Received 16 Aug 2010; revised 22 Sep 2010; accepted 28 Sep 2010; published 13 Oct 2010

In our experiments with the free standing samples, we found now two anomalous patterns: one placed close to the reflected ray and the other one in the transmission region but with a negative angle. These patterns showed illuminated and dark zones. These illuminated and dark zones correspond to the secondary waves, which either propagate within the allowed bands, or decay within the photonic band gaps, respectively. The number of rings in these patterns changes as a function of the angle of incidence and wavelength. This selective behavior could be useful for space filtering applications [11, 12], with the additional advantage that these p-Si structures are easily modified by varying the etching conditions, allowing to tune of such selective behavior [13].

2. One-dimensional porous silicon photonic structures.

The p-Si can be produced by electrochemical etching of crystalline Si in an HF solution. Anodization begins when a constant current is applied between the silicon wafer and the electrolyte [14]. Our multilayers were fabricated with p-type Si wafers (resistivity of 0.001-0.005 Ω-*cm* and (100) orientation), etched in an HF solution within a Teflon cell. The electrolyte was composed of HF, ethanol and glycerol in a volume ratio of 3:7:1. Before the electrochemical etching, on one side of the Si wafer an aluminum film was deposited and then heated at 550^0C during 15 min in a nitrogen atmosphere to make an electrical contact [13]. Because the electrochemical attack concentrates on the pore tip, by alternating the applied current, layers of different porosity and, as a consequence, different refractive indices can be produced [15]. The current density applied during the electrochemical etching of our samples was alternated from 1.5 mA/cm^2 (low porosity layer) to 40 mA/cm^2 (high porosity layer). We have experimentally measured the refractive indices of single p-Si layers, made under the same electrochemical conditions as the multilayers samples, from the interference fringes of their reflectance spectrum [16]. Reflectivity spectra of the samples were measured with a Shimadzu UV-3101 UV-VIS-NIR scanning spectrophotometer at 5^0 of incidence. Here we study a periodic structure containing 40 layers of low and high porosity. The thickness of each kind of layer was measured by scanning electron microscopy (SEM). The refractive indices in the structure are η_a=2.6 and η_b=1.4, for the low and high porosity layers of thickness a=300 nm and b=278.57 nm, respectively. The etching times are t_a= 333 s and t_b=14.9 s for the layer a and b, respectively. The half-Bragg relation between optical paths $\eta_b b = \eta_a a/2$ is satisfied in our structure [17]. In order to obtain free standing samples, after anodization, we abruptly increase the current density up to about $400mA/cm^2$ during 4 s [18]. After, the sample is submerged in ethanol during 10 minutes. The sample floats in ethanol, although sometimes it requires the use of a cutter to free it. Then, the previously dried free standing sample is located in a holder which is a plastic frame. The thickness of a typical p-Si free standing sample is around $12\mu m$. We can appreciate from the reflectivity spectrum (Fig. 1) that the photonic bands are well defined. However, interfaces between layers are not completely smooth, as it can be observed in the SEM images (Fig. 2). This fact influences the behavior of the transmitted light in p-Si multilayers, as it will be discussed below.

3. Study of the outcoming light of a p-Si Bragg mirror

Once we obtained the p-Si multilayers samples, we characterized the behavior of the transmitted and reflected light through these systems. The setup of our experiment is shown in Fig. 3, where light enters at different incidence angles with respect to the normal of the multilayer system. The p-Si multilayer sample was illuminated by a pulsed tunable laser (Component 1, PG401/SH EKSPLA), which allows us to choose a specific wavelength. The light was redirected to the sample by using a set of mirrors (Component 2, 66415, Oriel). The sample was placed on a system of two rotating stages (Component 8, 488 Newport) in order to select the

#133401 - $15.00 USD Received 16 Aug 2010; revised 22 Sep 2010; accepted 28 Sep 2010; published 13 Oct 2010

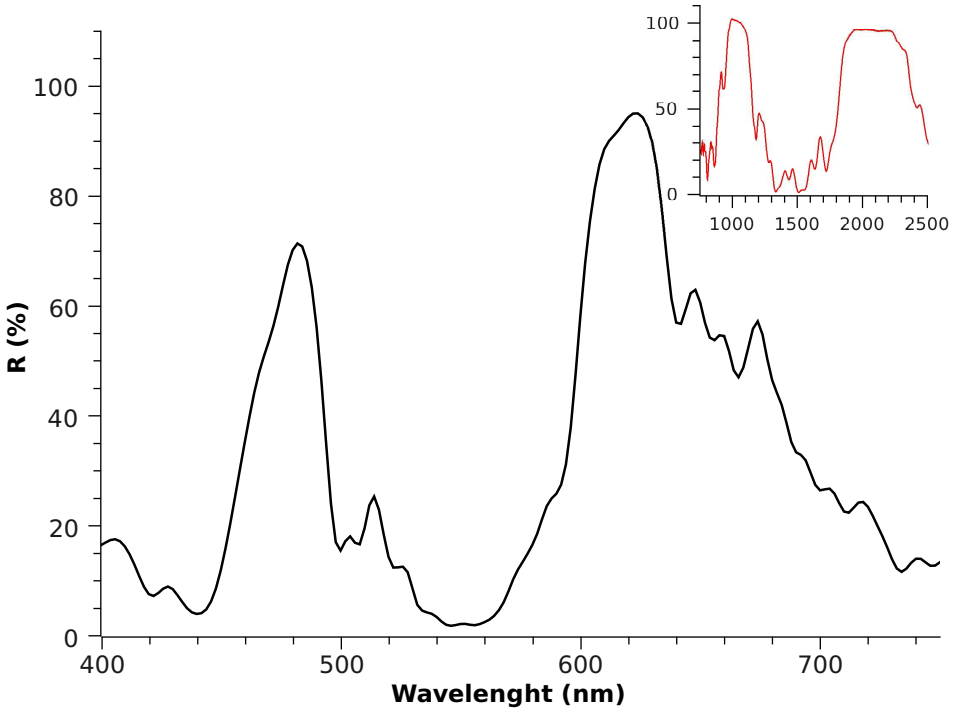

Fig. 1. Reflectivity of the p-Si multilayer showing two stop bands in the spectral range of visible light with the experimental conditions described in this section. The inset shows reflectivity spectrum of another pSi-sample designed to have stop bands in the infrared range.

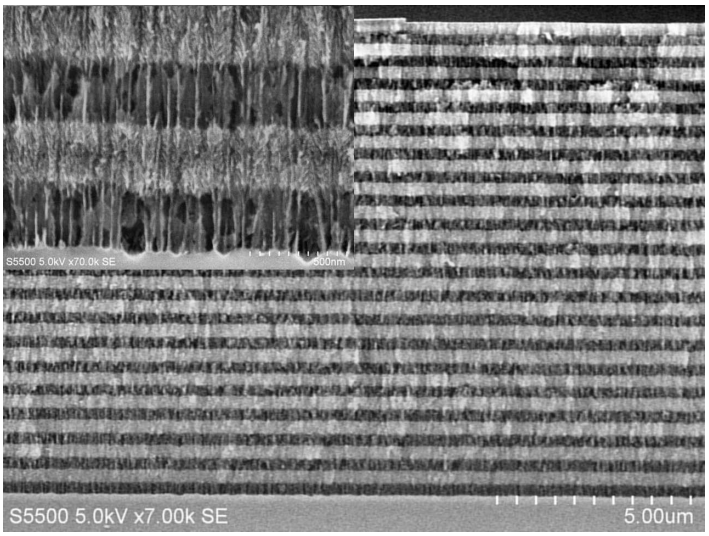

Fig. 2. SEM images of a p-Si multilayer as prepared.

#133401 - $15.00 USD Received 16 Aug 2010; revised 22 Sep 2010; accepted 28 Sep 2010; published 13 Oct 2010

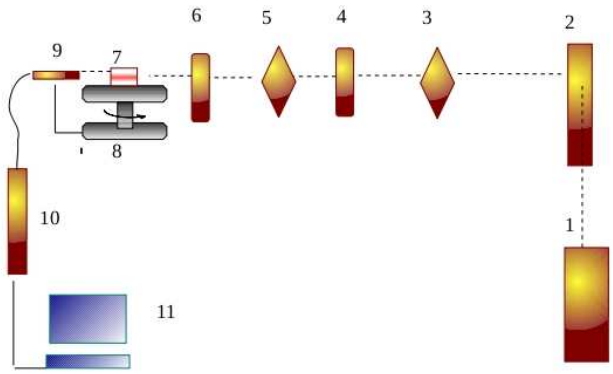

Fig. 3. A schematic design of our experimental setup for the transmission measurements. (1) Tunable pulsed laser, (2) Set of mirrors, (3) Polarizer, (4) Waveplate lambda/2, (5) Polarizer, (6) Diaphragm of 1 mm of diameter, (7) Free standing sample of p-Si, (8) Arrangement of two rotary stages, (9) Optical fiber, (10) Spectrophotometer, (11) Computer.

angle of incidence of the incoming light. The angular resolution in the rotatory system is 2 degrees. To collimate the size of the incident beam of light, a diaphragm of 1 mm of diameter (Component 6, Newport) was located at 2 cm of the sample. To detect the light, an optical fiber was placed in the inferior rotary stage (Component 9, P1000-2-UV-VIS, Ocean Optics), which let us scan the intensity of the light coming out at different angles. The optical fiber was connected to a spectrophotometer (Component 10, USB 2000+ Ocean Optics). The TE or TM polarization was selected by using two linear polarizers and a waveplate lambda/2 (Components 3, 5 and 4, respectively 10GL08, Newport). The light intensity measurements were collected in a computer (Component 11) connected to the spectrophotometer. We have specifically scanned the wavelength range from 580 to 630 nm in steps of 10 nm. This wavelength range includes the fourth photonic band gap and parts of the 3rd and 4th allowed photonic bands of our p-Si Bragg mirror. The range of the measured incidence angles goes from 5^0 to 60^0 in steps of 5^0, for each wavelength.

4. Results and discussion

Besides the expected reflected and transmitted rays, we clearly observed a couple of anomalous rays (Fig. 4). These rays formed a kind of interference pattern. The pattern center of both anomalous rays was located close to the normal direction of the plane of the sample. The anomalous reflected ray was found in the direction of the ordinary reflected ray, while the anomalous transmitted ray light was observed in the opposite direction to the ordinary refracted ray. This effect was observed in the range of angles from 25^0 to 60^0. The optimum angle to appreciate this phenomenon was 40^0. When these rays were projected on a screen in the far-field regime, it could be seen that they were composed of several co-focal rings, as it is schematically shown in front of Fig. 4. The number of rings depends on the angle of incidence and the wavelength. Fig. 5 shows the change observed in the interference pattern as a function of the

#133401 - $15.00 USD Received 16 Aug 2010; revised 22 Sep 2010; accepted 28 Sep 2010; published 13 Oct 2010

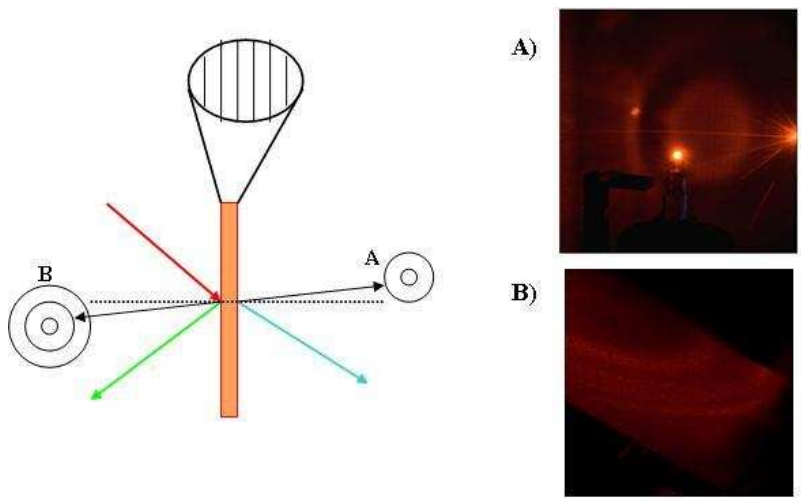

Fig. 4. Schematic representation of the light coming out from the p-Si multilayers. It shows the incident (red line), reflected ray (green line) and the refracted (blue line) rays. Part A) corresponds to the anomalous transmitted pattern, while part B) to the anomalous reflected pattern.

wavelength for the anomalous transmitted ray. In order to explain this surprising effect we have explored different possibilities. First, the negative refraction is not expected to occur in this experimental geometry, and it may not be a cause of the observed anomalous pattern. We note however, that in the case of negative refraction the refracted beam would go out of the sample on the opposite side from the normal direction with respect to the conventional transmitted light, which is indeed observed in our experiment. It is also clear that it is not a nonlinear effect, as the laser fluence measured at the entrance to the sample has an average value of 29.28 W/m^2, which is too low to induce nonlinear contributions [19]. Therefore, we argue that the causes for the rings that we observed are two: the elastic scattering of light inside the 1D PC of p-Si and the wave vectors selection of the scattered light performed by the photonic bands. If the multiple layers of our system were completely smooth (see Fig. 2), these anomalous scattered light would not be seen. However, there is an inevitable roughness at the interfaces between the layers of different porosity, which scatters elastically the transmitted light. The scattered light goes then in all directions, with its frequency conserved (Rayleigh scattering). Nevertheless, it can have all values of the in-plane component of the wave vector between 0 and the wave vector of the incident light k. Only the modes which have the values of k within the allowed photonic bands may propagate and eventually leave the p-Si multilayer. Those components of the scattered light which fall into photonic gaps cannot propagate and are filtered out. For wavelengths close to the band edge of one of the upper photonic bands, a ring structure of secondary emission appears. From this qualitative analysis, we conclude that we have observed a pattern related to the in-plane band structure of our 1D PC of p-Si.

To proceed with a quantitative analysis of the effect, in Fig. 6 we show the in-plane band structure of a 1D PC of p-Si, prepared as described in Section 2, in TE polarization. Here, we considered the relation of the frequency ω as a function of β in units of c/Λ, where c is the velocity of light and $\Lambda = a + b$ is the period of the Bragg mirror of p-Si, here a and b are the thickness of the low and high porosity layers, respectively. The values of β correspond to the in-plane component of the wave vector k, in units of $1/\Lambda$. We used a typical dispersion relation

#133401 - $15.00 USD Received 16 Aug 2010; revised 22 Sep 2010; accepted 28 Sep 2010; published 13 Oct 2010

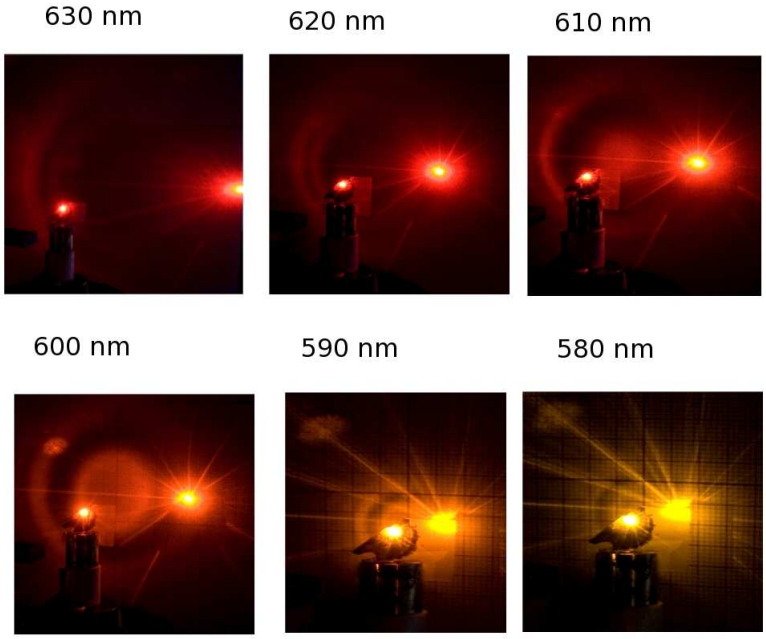

Fig. 5. Interference patterns of anomalous transmitted light at different wavelengths, for an angle of incidence of 40 in TE polarization.

for a periodic layer medium [20]. If we study the constant frequency line at $\omega = 6c/\Lambda$ (i. e. 600 nm), corresponding to the image in the right part of Fig. 6 taken in the transmission geometry at the wavelength of 600 nm and angle of incidence of 40^0, we can readily reconstruct the observed ringed structure. One can see that, at this wavelength and low angles, light propagates poorly since it is into the edge of the 4th allowed band (shown by color). At higher angles, it propagates freely within the 4th allowed band, which is responsible for the inner ring that we observe. The dark ring corresponds to the photonic gap between the 3rd and the 4th allowed bands, and the second bright ring corresponds to the 3rd allowed band. A similar behavior was observed in TM polarization (Fig. 7), but the intensity of the transmitted light was lower, the allowed photonic bands in TM polarization are quite narrow. The intensity of the secondary emission as a function of the detection angle is shown in Fig. 7 for TE and TM polarizations. In both polarizations we have observed two maxima, which correspond to the inner and outer two rings in the observed pattern. The negative values of the angles, shown at the horizontal axis of Fig. 7, indicate that the emission has been detected on the other side of the normal to the plane of the sample with respect to the conventional refraction. This kind of behavior was observed in all of our experiments, which were performed on several samples grown under similar conditions. Similar patterns have been reported for three dimensional PC's [21], but in that case they do not show multiple anomalous rays. In the inset of the Fig. 7, we show the normalized spatial power distribution due to the photonic structure: the experimental distribution and a finite element simulation (COMSOL 3.4) of the same distribution. The simulation is done for an ideal 1D-PC

#133401 - $15.00 USD Received 16 Aug 2010; revised 22 Sep 2010; accepted 28 Sep 2010; published 13 Oct 2010

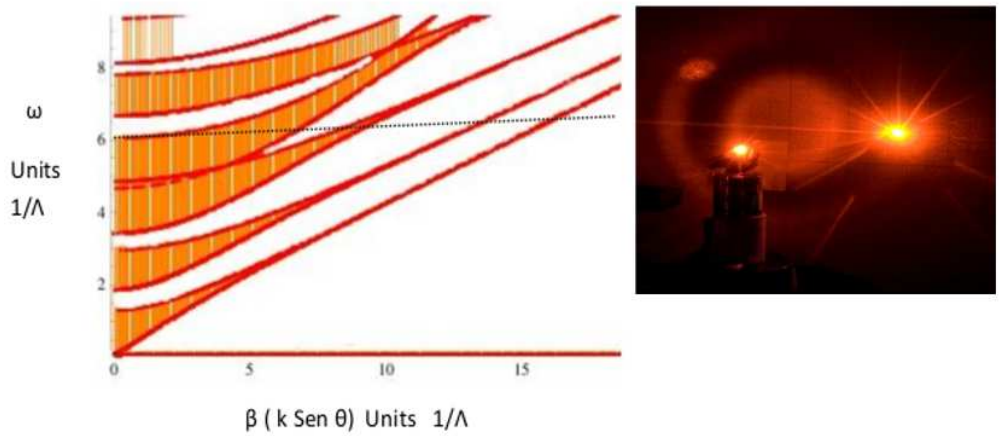

Fig. 6. In-plane photonic band structure of a 1D PC of p-Si, prepared as described in Section 2, in TE polarization. The scattered light travels at different angles finding allowed (color zones) and forbidden bands (white zones). The constant line corresponds to ω=6 (600 nm). Only the modes which propagate within allowed bands can leave the sample, which is why the observed pattern of secondary emission appears (inset).

and it uses the same refractive indices, thickness and number of layers as our experiments (TE polarization). In the simulation, we scanned incidence angles ranging from 0^0 to 45^0 degrees to have the same angular bandwidth as in the experiments. The power distribution is calculated at the structure output and the output angle value is obtained (with a maximum error of 5%) for each incidence angle. Qualitatively, the simulation shows a similar spatial power distribution, which indicates that the secondary emission spectra we have observed is due to the photonic band structure.

5. Final remarks

In summary, we have observed anomalous transmission and reflection of light through a porous silicon Bragg mirror, at the wavelengths corresponding to the edge of its fourth allowed photonic band. These anomalous rays form co-focal rings close to the normal to the sample. The number of rings in each pattern is a function of the wavelength. These anomalous patterns are present for a range of incidence angles going from 25^0 to 60^0. This anomalous behavior is related to the combined effect of scattering of light by the inhomogeneities of our periodical photonic structure and of spectral filtering of the scattered light by the photonic bands. This observation points out the importance of the effects of the imperfections in the behavior of light near the edges of the photonic bands in PC's. The anomalous reflected pattern could be useful for applications in optical devices [11]. Due to their selective behavior, both anomalous signals can be used for optical filtering of light. The simplicity of our structure and the possibility of modifying the band structure by just adjusting the etching parameters, offers the possibility of studying this phenomenon at different wavelengths, including the infrared region (see inset of Fig. 1).

#133401 - $15.00 USD Received 16 Aug 2010; revised 22 Sep 2010; accepted 28 Sep 2010; published 13 Oct 2010

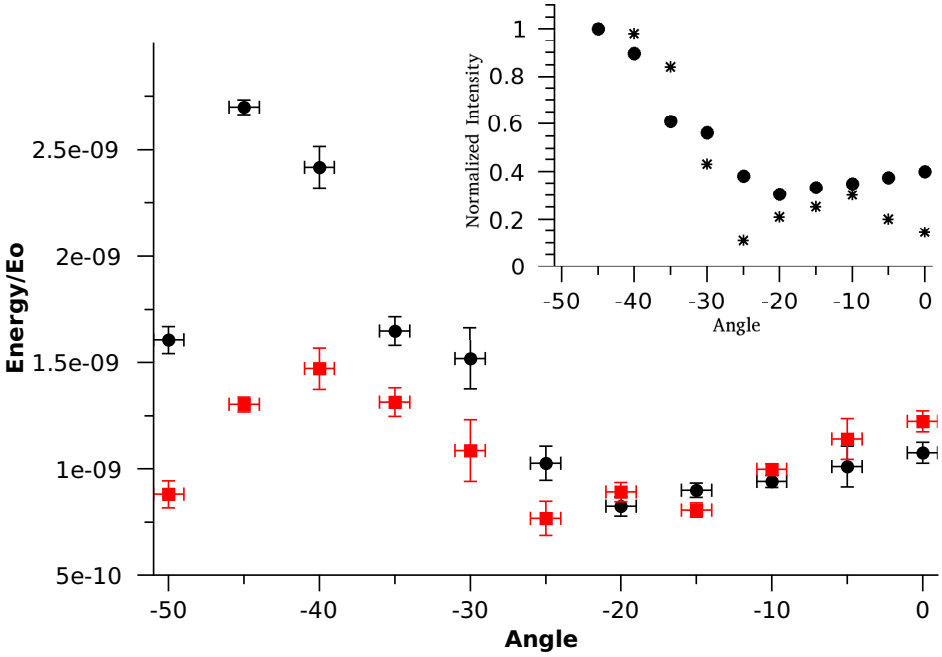

Fig. 7. The intensity of the outcoming light as a function of the detection angle for ω=6 (600 nm), for TE (black) and TM (red) polarization. The angle of incidence is 40^0. In inset we present the comparison between simulation (*) and experiments (•) for TE.

Acknowledgments

We acknowledge the work of José Campos for SEM images and Roberto Gleason for technical support in the optical experiments. We also acknowledge the financial support from PAPIIT-UNAM through grants IN106510 and IN108510 and from CONACyT through grant 80019. M. B. de la Mora acknowledges financial support from CONACyT through scholarship 202231. We thank also the support from EU ITN CLERMONT4 grant and the University of Rome II. J. E. Lugo and J. Faubert thank the support of NSERC-Essilor Research Chair and an NSERC operating grant.